

# Bound electronic and free carrier nonlinearities in Silicon nanocrystals at 1550nm

R. Spano<sup>1,\*</sup>, N. Daldosso<sup>1</sup>, M. Cazzanelli<sup>1</sup>, L. Ferraioli<sup>1</sup>, L. Tartara<sup>2</sup>, J. Yu<sup>2</sup>, V. Degiorgio<sup>2</sup>, E. Jordana<sup>3</sup>, J. M. Fedeli<sup>3</sup>, and L. Pavesi<sup>1</sup>

<sup>1</sup> Nanoscience Laboratory, Dipartimento di Fisica, Università di Trento, Via Sommarive 14, I-38050 Povo-Trento, Italy

<sup>2</sup> Dipartimento di Elettronica, Università degli Studi di Pavia, Via Ferrata 1, Pavia, I-27100, Italy

<sup>3</sup>CEA-LETI, 17, rue des Martyrs, Grenoble Cedex 9, 38054, France

\*Corresponding author: [spano@science.unitn.it](mailto:spano@science.unitn.it)

**Abstract:** We present a detailed investigation of the different processes responsible for the optical nonlinearities of silicon nanocrystals at 1550 nm. Through z-scan measurements, the bound-electronic and excited carrier contributions to the nonlinear refraction were measured in presence of two-photon absorption. A study of the nonlinear response at different excitation powers has permitted to determine the change in the refractive index per unit of photo-excited carrier density  $\sigma_f$  and the value of the real bound-electronic nonlinear refraction  $n_{2be}$  as a function of the nanocrystals size. Moreover at high excitation power, a saturation of the nonlinear absorption was observed due to band-filling effects.

©2009 Optical Society of America

**OCIS codes:** (190.0190) Nonlinear optics; (190.4720) Optical nonlinearities of condensed matter

---

## References and links

1. G. Vijaya Prakash, M. Cazzanelli, Z. Gaburro, L. Pavesi, F. Iacona, G. Franzò, and F. Priolo, "Nonlinear optical properties of silicon nanocrystals grown by plasma-enhanced chemical vapor deposition", *J. Appl. Phys.* **91**, 4607-4610 (2002).
2. S. Hernández, P. Pellegrino, A. Martínez, Y. Lebour, B. Garrido, R. Spano, M. Cazzanelli, N. Daldosso, L. Pavesi, E. Jordana, and J. M. Fedeli "Linear and non-linear optical properties of Si nanocrystals in SiO<sub>2</sub> deposited by PECVD", *J. Appl. Phys.* **103**, 064309 (2008).
3. L. Pavesi and G. Guillot (Eds.), *Optical interconnects*, Springer Series in Optical Sciences **119**.
4. P. Sanchis, J. Blasco, A. Martínez and J. Martí, "Design of Silicon-Based Slot Waveguide Configurations for Optimum Nonlinear Performance", *J. Lightwave Technol.* **25**, 1298-1305, (2007).
5. P. Sanchis, F. Cuesta-Soto, J. Blasco, J. García, A. Martínez, J. Martí, F. Riboli, and L. Pavesi, "All-optical MZI XOR logic gate based on Si slot waveguides filled by Si-nc embedded in SiO<sub>2</sub>", *Group IV Photonics. 3rd IEEE International Conference on*, 81-83 (2006).
6. A. Martínez, J. Blasco, P. Sanchis, R. Spano, J. V. Galán, J. García, J. M. Martínez, E. Jordana, P. Gautier, Y. Lebour, R. Guider, P. Pellegrino, S. Hernández, N. Daldosso, B. Garrido, J. M. Fedeli, L. Pavesi, and J. Martí, "Ultrafast all-optical switching on a CMOS silicon chip" submitted to *Nat. Photonics*.
7. L. Ferraioli, P. Bellutti, N. Daldosso, V. Mulloni, and L. Pavesi, "Nitrogen Influence on the Photoluminescence Properties of Silicon Nanocrystals", *Mater. Res. Soc. Symp. Proc.* **958**, 0958-L07-10.
8. F. Iacona, G. Franzò, and C. Spinella, "Correlation between luminescence and structural properties of Si nanocrystals", *J. Appl. Phys.* **87**, 1295-1303 (2000).
9. F. Iacona, C. Bongiorno, C. Spinella, S. Boninelli, and F. Priolo, "Formation and evolution of luminescent Si nanoclusters produced by thermal annealing of SiO<sub>x</sub> films" *J. Appl. Phys.* **95**, 3723-3732 (2004).
10. M. Sheik-Bahae, A. A. Said, T.-H. Wei, D. A. Hagan, and E. W. Van Stryland, "Sensitive Measurements of Optical Nonlinearities Using a Single Beam" *IEEE J. Quantum Electron.* **26**, 760-769 (1990).
11. R. Spano, M. Cazzanelli, N. Daldosso, Z. Gaburro, L. Ferraioli, L. Tartara, J. Yu, V. Degiorgio, S. Hernandez, Y. Lebour, P. Pellegrino, B. Garrido, E. Jordana, J. M. Fedeli, and L. Pavesi, "Non-linear optical properties of Si Nanocrystals", *Mater. Res. Soc. Symp. Proc.* **958**, L08-06(2007).
12. Q. Lin, J. Zhan, G. Piredda, R.W. Boyd, P. M. Fauchet, G. P. Agrawal, "Dispersion of silicon nonlinearities in the near infrared region", *Appl. Phys. Lett.* **91**, 021111 (2007).
13. R. L. Sutherland (Ed.), *Handbook of Nonlinear Optics* (Marcel Dekker, New York, 2003), pp. 465, 688.
14. R. Adair, L.L. Chase, and S. Payne, "Nonlinear refractive index of optical crystals", *Phys. Rev. B* **39**, 3337-3350, (1989).

15. W. P. Zang, J. G. Tian, Z.B. Liu, W. Y. Zhou, C. P. Zhang, and G. Y. Zhang, "Study on Z-scan characteristics of cascaded nonlinear media" *Appl. Phys. B* **77**, 529-533 (2003).
16. D. O. Caplan G. S. Canter, and P. Kumar, "Characterization of dynamic optical nonlinearities by continuous time-resolved Z-scan", *Opt. Lett.* **21**, 1342-1344, (1996).
17. C. Garcia, B. Garrido, P. Pellegrino, R. Ferre, J. A. Moreno, J. R. Morante, L. Pavesi, and M. Cazzanelli, "Size dependence of lifetime and absorption cross-section of Si nanocrystals embedded in SiO<sub>2</sub>", *Appl. Phys. Lett.* **82**, 1595-1597 (2003).
18. Ö. Boyraz, P. Koonath, V. Raghunathan, and B. Jalali, "All optical switching and continuum generation in silicon waveguides" *Opt. Express* **12**, 4094-4102 (2004), [http://www.opticsinfobase.org/DirectPDFAccess/01BFA884-BDB9-137E-C3FEFCACD82C4E55\\_80903.pdf?da=1&id=80903&seq=0&CFID=3010471&CFTOKEN=82361634](http://www.opticsinfobase.org/DirectPDFAccess/01BFA884-BDB9-137E-C3FEFCACD82C4E55_80903.pdf?da=1&id=80903&seq=0&CFID=3010471&CFTOKEN=82361634)
19. A. A. Said, M. Sheik-Bahae, D. J. Hagan, T. H. Wei, J. Wang, J. Young, and E. W. Van Stryland, "Determination of bound-electronic and free-carrier nonlinearities in ZnSe, GaAs, CdTe, and ZnTe", *J. Opt. Soc. Am. B* **9**, 405-414 (1991).
20. K. Ogusu and K. Shinkawa, "Optical nonlinearities in silicon for pulse durations of the order of nanosecond at 1.06 μm", *Opt. Express* **16**, 14780-14791, (2008).
21. M. Dinu, F. Quochi, and H. Garcia, "Third-order nonlinearities in silicon at telecom wavelengths" *Appl. Phys. Lett.* **82**, 2954-2956 (2003).

## 1. Introduction

The advent of silicon photonics urges to find new nonlinear photonic materials to implement various key optical devices such as switches, routers, wavelength converters, etc..., which are to be silicon-compatible. Silicon nanocrystals (Si-nc) have the potentiality to play the role of the active material in such devices since they show relevant optical nonlinearities [1, 2] and are suitable for integration in silicon photonics since their fabrication is compatible with CMOS technology [3]. Recently published works, highlighted the peculiarity of Si-nc to have both low linear absorption and high nonlinear refraction properties and proposed to use Si-nc as active nonlinear elements in switching devices [4-6]. As most of the research on the nonlinearities in Si-nc has been performed at short wavelengths [1], the purpose of this paper is to carry out the first systematic investigation of the nonlinear properties of Si-nc at the technologically relevant 1550 nm wavelength. In particular, the correlation of the nonlinear response to the structural parameters of the material is studied. In addition, a great attention is devoted to the mechanisms involved in the nonlinear response, in order to isolate the effect of each different contribution.

## 2. Experimental details

Silicon rich silicon oxide (SRSO) films were deposited by plasma enhanced chemical vapor deposition (PECVD) on a quartz substrate using N<sub>2</sub>O and SiH<sub>4</sub> as precursor gases [2]. Four series of samples were deposited having silicon excess of 5, 8, 20 and 24 at. % as determined by XPS (X-Ray Photoelectron Spectroscopy) measurements. After the deposition, a 1 hour long annealing treatment was performed in N<sub>2</sub> at three different temperatures (800, 1100 and 1250 °C). Consequently, Si-nc were developed. Depending on the annealing temperature, the size and the crystalline state of Si-nc varied: it is well known that the increase of the annealing temperature determines the increase of the size and the crystallization of Si-nc [7-9]. Energy-filtered transmission electron microscopy (EFTEM) measurements allowed to evaluate the Si-nc average diameters being 4.8, 3.9 and ~1 nm for the samples with a silicon excess of 24, 20 and 8 at. %, respectively, and annealed at 1250°C [2]. The structural parameters, such as the linear refractive index  $n_0$ , the extinction coefficient  $k$  and the thickness  $L$ , were determined by the ellipsometric technique and are reported in Table 1 for the as-deposited samples.

The nonlinear coefficients of Si-nc were measured by the Z-scan technique [10]. The light source was an optical parametric generator (OPG) pumped by an amplified Ti:Sapphire laser system at a 1-kHz repetition rate with 100-fs long pulses at 1550 nm. We resorted to such a source to measure the fast nonlinear response of the material and to avoid thermal lensing effects which might arise from high repetition rate and/or long pulse duration [11].

Table 1. Linear parameters at 1550 nm with respect to the Silicon excess ( $Si_{exc}$ ).  $n_0$  refers to the linear refractive index,  $k$  to the extinction coefficient,  $\alpha$  to the absorption coefficient and  $L$  to the sample thickness.

Sample	$Si_{exc}$ (at. %)	$n_0$	$k$	$\alpha$ ( $cm^{-1}$ )	$L$ (nm)
A	5	1.46	$<10^{-5}$	0.81	660
B	8	1.54	$<10^{-5}$	0.81	590
C	20	1.81	$<10^{-5}$	0.81	559
D	24	1.89	$<10^{-5}$	0.81	522

To take into account the substrate contribution, two reference samples were measured: a 300- $\mu$ m thick crystalline  $SiO_2$  sample and a 2-mm thick amorphous  $SiO_2$  sample. The measured  $n_2$  values were  $(1.8 \pm 0.25) \times 10^{-16} cm^2/W$  and  $(2.3 \pm 0.8) \times 10^{-16} cm^2/W$  for the crystalline and for the amorphous samples, respectively, in agreement with the literature data [13, 14]. The phase shift due to the  $SiO_2$  substrate was subtracted from the measured one by using the procedure known in literature for multilayered structures [15].

Z-scan was performed both in closed and open aperture configurations (Fig. 1 and 2). To analyze the z-scan trace in closed aperture configuration and extract the nonlinear coefficients, we used the equation reported in [12] providing the transmittance  $T_{cl}$  of the sample:

$$T = 1 - 4B \frac{(x^2 + 3)}{(x^2 + 9)(x^2 + 1)} + \frac{8\Delta\phi x}{(x^2 + 9)(x^2 + 1)}. \quad (2)$$

Where  $\Delta\phi$  is the nonlinear phase shift,  $B$  is related to  $\beta$ , the non linear absorption coefficient,  $x = z/z_0$  is the ratio between the position of the sample  $z$  and the Rayleigh length  $z_0$ .

The nonlinear refractive index  $n_2$  is related to  $\Delta\phi$  and  $\beta$  is related to  $B$  by the usual formula [11]:

$$B = \frac{\beta I_0 L_{eff}}{2\sqrt{2}}, \quad (3)$$

$$\Delta\phi = \frac{2\pi I_0 L_{eff}}{\lambda\sqrt{2}} n_2.$$

Where  $\alpha$  is the linear absorption coefficient at the wavelength  $\lambda$ ,  $L_{eff} = \frac{(1 - e^{-\alpha L})}{\alpha}$  is the effective length,  $L$  is the sample thickness and  $I_0$  is the peak intensity. For open aperture z-scan measurements, we used [12]:

$$T_{op} = 1 - \frac{B}{1 + x^2}. \quad (4)$$

It should be noted that the value of  $B$  extracted by the closed aperture scan is coincident with the one extracted by the open aperture scan, within the error bars (see analysis reported in Fig. 1 and 2).

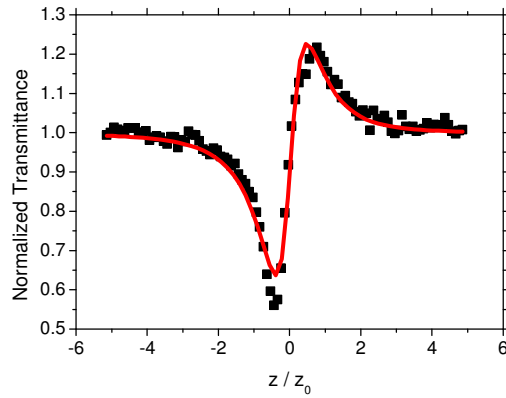


Fig. 1. Closed aperture z-scan trace recorded from sample A annealed at  $T = 800^\circ\text{C}$  and excited at  $I_0 = (1.05 \pm 0.4) \times 10^{12} \text{ W/cm}^2$ . The beam waist was measured by knife edge technique and was  $w_0 = 23 \mu\text{m}$ . The red curve is the result of the fit with Eq. (1). From the fit we obtained a total nonlinear phase shift (quartz substrate and Silicon nanocrystals layer)  $\Delta\phi = (0.72 \pm 0.02)$  and a nonlinear absorption parameter  $B = 0.08 \pm 0.01$ . The resulting nonlinear refractive index is  $n_2 = (1.03 \pm 0.4) \times 10^{-13} \text{ cm}^2/\text{W}$  and nonlinear absorption is  $\beta = (4.4 \pm 1.5) \times 10^{-10} \text{ cm/W}$ .

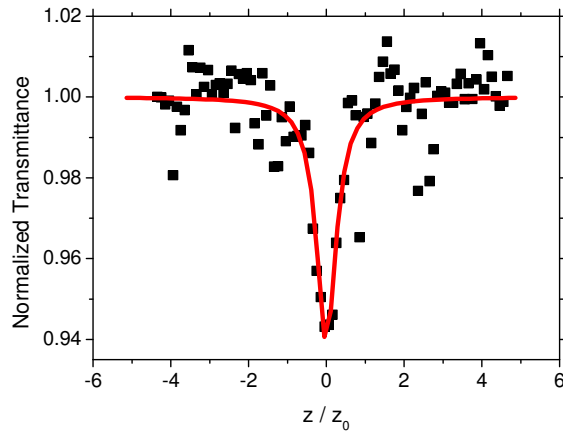


Fig. 2. Open aperture z-scan trace recorded from sample A annealed at  $T = 800^\circ\text{C}$ , and excited at  $I_0 = (9 \pm 3) \times 10^{11} \text{ W/cm}^2$ . The red curve is the result of the fit with Eq. (4). From the fit we obtained the total nonlinear absorption (quartz substrate and Silicon nanocrystals layer)  $B = 0.06 \pm 0.01$ , the resulting nonlinear absorption is  $\beta = (2.4 \pm 0.7) \times 10^{-10} \text{ cm/W}$ .

Because the aim of this paper is to determine the sign and magnitude of the nonlinear refraction, which can be extracted only via closed aperture z-scan, and in order to reduce the number of measurements, we performed only closed aperture z-scan measurements to obtain both nonlinear refraction and nonlinear absorption. Figure 3 reports one measurement at low power levels with a small phase shift.

The error bars on the non linear parameters  $n_2$  and  $\beta$  are obtained by propagating the errors:

$$\Delta n_2 = n_2 \left( \frac{\Delta(\Delta\phi)}{(\Delta\phi)} + \frac{\Delta P_{AVE}}{P_{AVE}} + \frac{2\Delta w_0}{w_0} \right) \quad (5)$$

where  $\Delta(\Delta\varphi)$  is the error on the phase shift arising from the fitting procedure and  $\Delta P_{AVE}$  is the fluctuation of the average power  $P_{AVE}$  measured during the z-scan experiment, which is directly related to the peak intensity  $I_0$ ,  $\Delta w_0$  is the fluctuation of the beam waist .

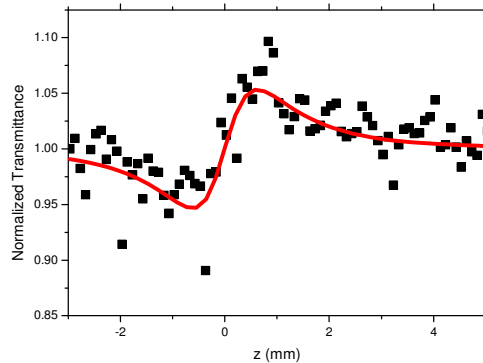


Fig. 3. Closed aperture z-scan trace recorded from sample B annealed at  $T=1100^{\circ}\text{C}$ , and excited at  $I_0=(2.3\pm 0.8)\times 10^{11}\text{W}/\text{cm}^2$ . The red curve is the result of the fit with Eq. (2). From the fit we obtain the nonlinear phase shift (quartz substrate and Silicon nanocrystals layer)  $\Delta\varphi=(0.13\pm 0.01)$  and a nonlinear absorption parameter  $B=0$ , the resulting nonlinear refractive index is  $n_2=(4\pm 2)\times 10^{-14}\text{cm}^2/\text{W}$ .

Moreover the z-scan measurements revealed a power threshold, behind which it is not possible to record any z-scan trace, and this threshold depends on the sample under study. Although the power used for the z-scan measurements can appear extremely high, it is worth to note that at 1550nm the linear absorption is very low, as reported in Table 1, and the short pulse duration avoids any significant sample damage.

### 3. Results

Figure 4 reports the dependence of  $n_2$  on the Si excess in the films for the various annealing temperatures and for high and low peak intensities.

At low peak intensities,  $n_2$  does not depend on the silicon content and the annealing temperature, while at a high peak intensities  $n_2$  decreases as the silicon content and the annealing temperature increase. The decrease is so strong to turn  $n_2$  negative in some samples. We think that this is due to the excited carriers generated by two-photon absorption in Si-nc. According to our data, carriers are generated more effectively in samples having higher silicon content and annealed at higher temperatures, i.e. the more crystalline ones. Two-photon absorption processes excite carriers in the Si-nc which, in turn, induce a change of the refractive index, an effect well depicted by Kramers-Kronig relations. This contribution to  $n_2$  is referred to as a free carrier effect in bulk materials [13, 19], and show up as a negative contribution to the nonlinear refractive index. If we consider this, we can explain why  $n_2$  decreases at high intensities eventually becoming negative. It is worth to note that for a few samples the effect is so strong to completely deform the z-scan trace in such a way that no reliable data can be obtained. The data of these samples are omitted in Fig. 4.

Since carrier generated in Si-nc are not free to move, we will refer to it as an excited carrier effect.

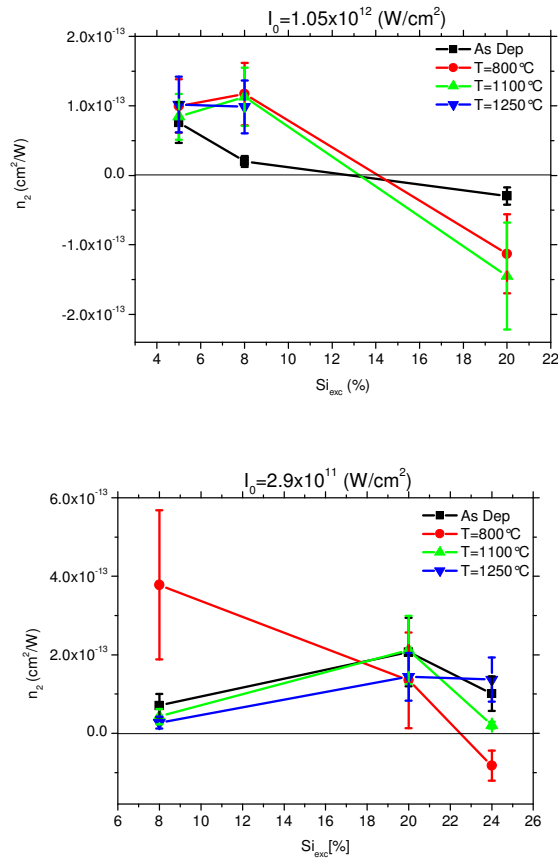


Fig. 4. Nonlinear refractive index measured at a high (top) and a low (bottom) peak intensity as a function of the Si excess for different annealing temperatures. The data for the 24% silicon excess sample have been omitted in the top plot since this sample shows a distorted z-scan trace when pumped at high intensities. In addition, the data for the 5% silicon excess sample are absent in the bottom plot since the z-scan trace at low power excitation was too weak to extract reliable nonlinear coefficients.

In order to quantify the effects of carrier generation in Si-nc, we used a simple model based on a rate equation to compute the carrier density  $\Delta N$  generated by two-photon absorption [16]:

$$\frac{\partial \Delta N}{\partial t} = \frac{\beta I_0^2}{2\hbar\omega} - \frac{\Delta N}{\tau}. \quad (5)$$

Where  $\frac{\beta I_0^2}{2\hbar\omega}$  is the generation term due to two photon absorption,  $\hbar\omega$  is the photon energy, and  $\tau = 100 \mu\text{s}$  is the exciton recombination lifetime in Si-nc [17]. The exact value of the recombination lifetime is not relevant as long as it is longer than the excitation pulse duration. The equation was numerically solved by considering a 100-fs long Gaussian excitation pulse.  $\Delta N$  was used to have an estimation of the excited carrier nonlinear refraction, by using [18]:

$$n_{2exc} = -\frac{e^2 \lambda^2}{8\pi^2 c^2 \epsilon_0 n_0} \left( \frac{1}{m_{ce}^*} + \frac{1}{m_{ch}^*} \right) \frac{\Delta N}{I_0} \quad (6),$$

where  $\epsilon_0$  is the vacuum permittivity,  $m_{ce}^*$  and  $m_{ch}^*$  are the effective masses of the electron and of the hole respectively, assumed to be the same as in silicon. The results we obtained are reported and compared to the experimental data in Table 2 for sample B.

Table 2. Comparison of the experimental results with the simulation data for sample B having a 8 at. % Si excess and annealed at T = 800°C . The  $\beta$  and  $n_2$  values are extracted from the z-scan measurements while the last column gives  $n_{2exc}$  computed with eq. (6).

$I_0$ (W/cm <sup>2</sup> )	$\beta$ (cm/W)	$n_2$ (cm <sup>2</sup> /W)	$n_{2exc}$ (cm <sup>2</sup> /W)
$5 \times 10^{11}$	$6.7 \times 10^{-9}$	$(4 \pm 2) \times 10^{-13}$	$-2.06 \times 10^{-14}$
$2.15 \times 10^{12}$	$3.1 \times 10^{-9}$	$-(2.1 \pm 0.9) \times 10^{-14}$	$-4.7 \times 10^{-14}$

Despite the simplicity of the model, the results are surprisingly in an extremely good agreement with the measured data. This clearly shows that at high intensities the nonlinear refraction in Si-nc is dominated by excited carrier effects.

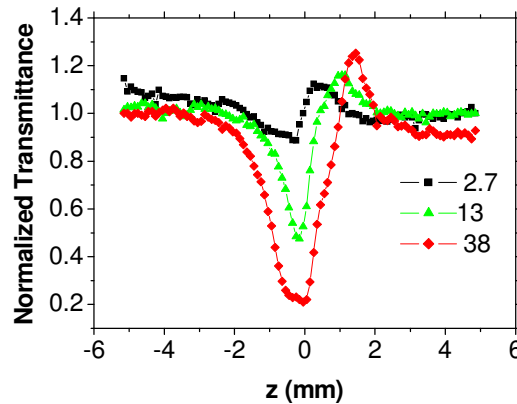


Fig. 5. Z-scan trace for the sample B, annealed at T=800°C, for different peak intensities (given as a label in the plot in unit of  $10^{11}$  W/cm<sup>2</sup>).

#### 4. Excited carrier effects

A study of the nonlinear response of Si-nc as a function of the peak intensity allows separating the excited carrier effect from the pure bound-electronic effect, which arises from the polarization of the electronic cloud around the atom. Although at high peak intensity the phase shift in the transmission trace is quite large and, even, the trace itself is deformed by two photon absorption, z-scan analysis can still be applied as discussed in [19]. Unfortunately we could carry out this kind of investigation only for a few values of the excess silicon content. In fact, in some samples, two photon absorption was so strong to deform completely the z-scan trace at high intensities, while in other samples the nonlinear refraction was so weak that no signal could be recorded at low peak intensities. As an example, in Fig.5 the z-scan traces for the sample B, annealed at T = 800°C, are reported. A fitting of the peak-intensity dependent data with Eq. (2) yields the results reported in Fig. 6.

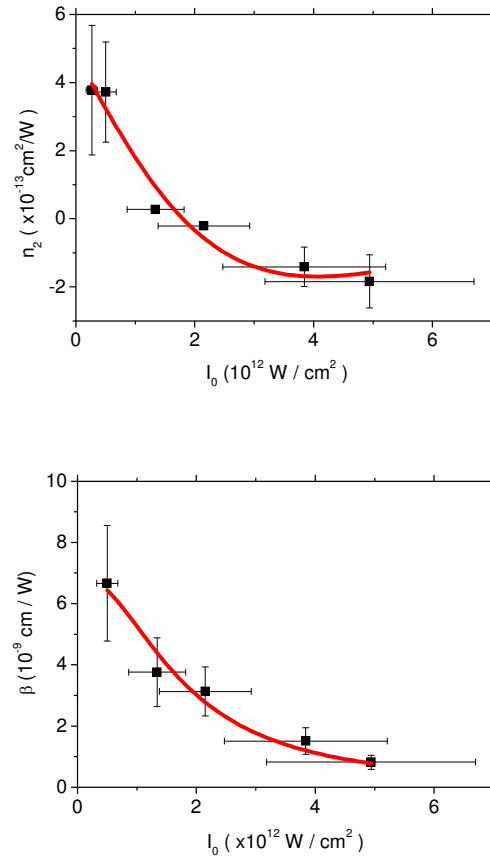


Fig. 6. Nonlinear refraction and absolute value of the nonlinear absorption from sample B annealed at 800°C. The data are fitted with Eq. (9) and Eq. (10).

The data show a decrease of both  $n_2$  and  $\beta$  as the peak intensity increases. In addition,  $n_2$  changes from positive to negative. This behavior can be explained as follows: at low peak intensities, the positive bound-electronic effect dominates the nonlinear response, whereas at high peak intensities the nonlinearities due to excited carriers overcome the bound-electronic ones. At high peak intensities we can observe a decrease of  $\beta$ , too.

In order to explain the decrease of  $\beta$ , we propose a phenomenological model. Because of the short duration of laser pulses (100 fs) with respect to the typical electron-phonon scattering time ( $\sim$  ps), the nanocrystals effectively behave as a two level system. Therefore, at high pumping excitation power, band filling effects can be observed [13]. The saturation in the excited carrier population is thus responsible for the bleaching of  $\beta$  (Fig. 6). In addition, saturation affects also the nonlinear refractive index, which flattens at high intensities. Similar conclusions were reached in a recent study on nonlinear refraction in bulk Silicon at 1.06  $\mu$ m [20].

A simple modeling allows separating the bound-electronic from the excited carrier contribution to the  $n_2$ . Let us write the change of the refractive index  $\Delta n$  as the sum of the bound-electronic contribution  $n_{2be}$  and of the contribution due to the excited carriers generated by two photon absorption [19]:

$$\Delta n = n_{2be} I_0 - \sigma_r N \quad (7),$$

where  $N$  is obtained by integrating Eq. (5) and the minus sign accounts for the negative contribution of excited carriers to the nonlinear refraction. If we further ignore excited carrier relaxation during the pulse excitation (carrier lifetime  $\gg$  pulse duration), then

$$N(I) = \frac{\beta}{2\hbar\omega} \int_{-\infty}^t I_0^2(t') dt' \quad (8),$$

where  $I_0(t)$  is the actual pulse temporal lineshape. The nonlinear absorption is expressed in terms of the saturation intensity  $I_s$  [13] as:

$$\beta = \frac{\beta_0}{1 + \left(\frac{I_0}{I_s}\right)^2}. \quad (9).$$

If the pulse lineshape is Gaussian, Eq. (8) can be easily integrated and Eq. (7) becomes:

$$\frac{\Delta n}{I_0} = n_2 = n_{2be} - \frac{C\sigma_r I_0}{1 + \left(\frac{I_0}{I_s}\right)^2} \quad (10),$$

where  $C \cong 0.14\beta_0 t_{FWHM} / \hbar\omega$ , with  $t_{FWHM} = 100\text{fs}$  the excitation pulse duration and  $\sigma_r$  the change in the refractive index per excited carrier [18]. A fit of the data reported in Fig. 6 by Eq. (9) and Eq. (10) allows extracting  $n_{2be} = (4.8 \pm 0.6) \times 10^{-13} \text{cm}^2/\text{W}$ ,  $\beta_0 = (7.0 \pm 0.6) \times 10^{-9} \text{cm}/\text{W}$ ,  $I_s = 4.07 \times 10^{12} \text{W}/\text{cm}^2$  and  $\sigma_r = (1.2 \pm 0.3) \times 10^{-22} \text{cm}^3$ . It is worth to note that the value of  $\sigma_r$  is similar to the one reported for other semiconductors [19].

By using this procedure, we have analyzed the various samples and we were able to extract  $n_{2be}$  as a function of the Si content and of the annealing temperature as reported in Fig. 7.

A trend for  $n_{2be}$  can be observed both as a function of the annealing temperature and of the silicon excess. In particular, a strong nonlinearity is observed for the sample annealed at low temperatures and with low silicon content. Low temperature and low silicon excess lead to small Si-nc. This is in agreement with former results reported in literature [1, 2] where quantum confinement was claimed to be responsible for the increase of  $n_2$  with decreasing the Si-nc sizes. As can be seen,  $n_{2be}$  decreases with increasing the annealing temperature approaching the as deposited value at  $T=1250^\circ\text{C}$ . This is quite surprising and show that Si-nc developed at  $1250^\circ\text{C}$  are too large to yield quantum confinement enhancement effect. In this material the nonlinearities are only due to the dielectric mismatch effects by which the different dielectric environments affect the Si polarizability due to the composite nature of the material.

## 5. Conclusions

By using femtosecond pulses we were able to isolate the various contributions to the optical nonlinear properties of Si-nc. A detailed investigation was carried out to highlight the role of excited carrier and bound-electronic effects as a function of the peak power. In particular, the nonlinear response arising from the bound-electronic polarization can be as high as  $\sim 10^{-13} \text{cm}^2/\text{W}$  for small Si-nc embedded in an amorphous  $\text{SiO}_2$  matrix. When larger Si-nc are formed either because of the high annealing temperature or because of the high Si excess in the as-deposited films, a negative nonlinear response is observed due to excited carrier generation following two-photon absorption. Moreover, the analysis of nonlinear refraction and absorption as a function of the peak intensity shows the saturation of the nonlinearity due to a band filling mechanism. For the present study the saturation intensity is  $\sim 10^{12} \text{W}/\text{cm}^2$ . It was

also found that the bound-electronic nonlinear response shows a dependence on the Si excess which can be ascribed to a quantum confinement effect.

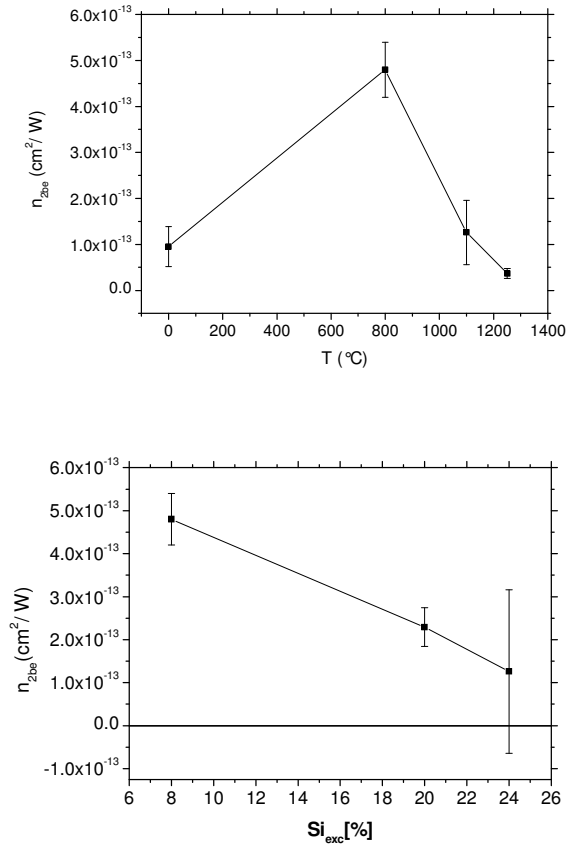


Fig. 7. Bound-electronic nonlinear response extracted from the non-linear refractive index by fitting the procedure depicted in Equation (10) as a function of annealing temperature for the sample B (top) and as a function of Silicon excess for samples annealed at  $T=800^\circ\text{C}$  (bottom). The temperature of the as deposited sample was labeled as  $T=0^\circ\text{C}$ , as a convention. The lines represent only a guide for the eyes.

Our results show that Si-nc have a nonlinear response one order of magnitude higher than that of bulk silicon [12], and three order of magnitude higher than that of silica [13]. The Si-nc nonlinear refraction is of the same order of magnitude of that of GaAs [21], with the main advantage of the CMOS compatibility. Viable applications of Si-nc can be found in all optical switching devices which, based on the bound nonlinear response, can have the potentiality to go beyond 40 Gbps [5, 6].

#### Acknowledgments

This work was supported by EC through the PHOLOGIC (FP6-017158) project. We acknowledge Prof. Blas Garrido and his group for the linear optical measurements.